

# Remote Changes in Cortical Excitability after Experimental Traumatic Brain Injury and Functional Reorganization

Derek R. Verley,<sup>1</sup> Daniel Torolira,<sup>1</sup> Brandon Pulido,<sup>1</sup> Boris Gutman,<sup>2</sup> Anatol Bragin,<sup>3</sup>  
Andrew Mayer,<sup>4</sup> and Neil G. Harris<sup>1</sup>

## Abstract

Although cognitive and behavioral deficits are well known to occur following traumatic brain injury (TBI), motor deficits that occur even after mild trauma are far less known, yet are equally persistent. This study was aimed at making progress toward determining how the brain reorganizes in response to TBI. We used the adult rat controlled cortical impact injury model to study the ipsilesional forelimb map evoked by electrical stimulation of the affected limb, as well as the contralesional forelimb map evoked by stimulation of the unaffected limb, both before injury and at 1, 2, 3, and 4 weeks after using functional magnetic resonance imaging (fMRI). End-point c-FOS immunohistochemistry data following 1 h of constant stimulation of the unaffected limb were acquired in the same rats to avoid any potential confounds due to altered cerebrovascular coupling. Single and paired-pulse sensory evoked potential (SEP) data were recorded from skull electrodes over the contralesional cortex in a parallel series of rats before injury, at 3 days, and at 1, 2, 3, and 4 weeks after injury in order to determine whether alterations in cortical excitability accompanied reorganization of the cortical map. The results show a transient trans-hemispheric shift in the ipsilesional cortical map as indicated by fMRI, remote contralesional increases in cortical excitability that occur in spatially similar regions to altered fMRI activity and greater c-FOS activation, and reduced or absent ipsilesional cortical activity chronically. The contralesional changes also were indicated by reduced SEP latency within 3 days after injury, but not by blood oxygenation level-dependent fMRI until much later. Detailed interrogation of cortical excitability using paired-pulse electrophysiology showed that the contralesional cortex undergoes both an early and a late post-injury period of hyper-excitability in response to injury, interspersed by a period of relatively normal activity. From these data, we postulate a cross-hemispheric mechanism by which remote cortex excitability inhibits ipsilesional activation by rebalanced cortical excitation-inhibition.

**Keywords:** excitability; fMRI; plasticity; recovery; sensorimotor

## Introduction

**M**OTOR DEFICITS AFTER TRAUMATIC BRAIN INJURY (TBI) are a significantly under-studied problem. Although it is well known that TBI results in severe and persistent cognitive and behavioral deficits in a many patients, motor weakness also occurs in 9–56% of injured individuals,<sup>1–5</sup> with up to 30% showing persistent deficits in upper limb function 2–5 years post-TBI.<sup>4,6</sup> These alterations in motor function are not merely restricted to severe TBI in adults since deficits in sensory-motor cortical inhibition have been measured in mild TBI over 1 year following a single or multiple concussions<sup>7</sup> and in children.<sup>8</sup> Persistent deficits in cortical functional activation evoked by finger tapping have been measured at 1 year after mild injury,<sup>9</sup> and electrophysiological data reveal significant motor system changes in athletes who sustained their injury almost 3

decades earlier.<sup>10</sup> Moreover, even despite good general recovery in patients 3–4 years following injury, abnormal movement-related cortical potentials remain.<sup>11</sup> It is clear, therefore, that persistent motor deficits are an important sequela of TBI, but unlike in stroke, they have received relatively little attention as far as clinical interventional strategies and experimental mechanistic research.

Much of basic research on traumatic brain injury (TBI) has been focused on neuroprotective strategies largely targeting the ipsilesional (injured) hemisphere. However, there is a great deal of clinical evidence, albeit after stroke injury and not TBI, to indicate that remote brain regions far removed from the primary site of injury, such as the contralesional hemisphere (the opposite, less-injured hemisphere) also are significantly affected, and that such remote changes may inhibit normal functioning of the injured side.<sup>12,13</sup> After TBI, metabolic diaschisis is observed and is likely

<sup>1</sup>UCLA Brain Injury Research Center, Department of Neurosurgery, <sup>3</sup>Department of Neurology, University of California, Los Angeles, California.

<sup>2</sup>Department of Neurology, Imaging Genetics Center, Keck/ University of Southern California School of Medicine, Institute for Neuroimaging and Informatics, University of Southern California, California.

<sup>4</sup>The MIND Research Network and Department of Neurology, University of New Mexico, Albuquerque, New Mexico.

one of a number of mechanisms responsible for functional metabolic changes in regions remote from a major injury site.<sup>14</sup> Prior work in the experimental controlled cortical impact injury (CCI) rat model of TBI has established that affected hindlimb-evoked cerebral blood flow is altered by TBI, and that contralesional activation occurs rather than the normal unilateral activity within the hemisphere opposite the stimulated limb.<sup>15</sup> This functional recruitment of remote regions has been shown to occur as early as 1–2 days after TBI in the rodent in association with impairments in phasic GABAergic transmission,<sup>16</sup> and with subsequent alterations in contralesional neuronal circuitry at more chronic time-points.<sup>17</sup> It remains unclear how these remote changes evolve after TBI and whether they play a significant part in restoration of function, or whether they are merely temporary adaptive changes that unfold to support short-term compensatory behavior until spontaneous resumption of some normal function occurs. In addition, wider questions remain about these remote changes, the timing of the start of neurorehabilitative care after TBI, and on which brain region to focus. These questions warrant an understanding of how mechanisms of plasticity evolve to govern motor function after injury.

The current study focused on making progress toward determining how the cortex reorganizes in response to injury as measured using forelimb evoked functional magnetic resonance imaging (fMRI) activity. Given the likelihood of altered neuronal-vascular coupling after TBI, and the unknown contribution of significant TBI-associated gliosis to the blood oxygen level-dependent (BOLD) signal, we also employed cortical electrophysiologic measurements as well as c-FOS histology. Current results indicate that the affected limb cortical map temporarily shifts to the contralesional side in accordance with the severity of injury, but then remains absent or reduced in all cortical regions at 4 weeks. BOLD signal changes were increased within the contralesional cortex at 4 weeks post-injury, and evidence from studying sensory-evoked potentials (SEPs) showed that this was accompanied by increased cortical excitability. We discuss these data in light of other post-injury data supporting excitability changes and we postulate a potential mechanism to explain the low or absent ipsilesional activity at chronic times.

## Methods

### Experimental protocol

Two separate cohorts of adult male rats were used to acquire either: 1) longitudinal sensory-evoked (fMRI) data before injury and then at 1, 2, 3, and 4 weeks after mild-to-moderate CCI ( $n=11$ ), followed by c-FOS histology in a subset of animals ( $n=8$ ) together with an additional seven injured rats at 5 weeks post-injury; or 2) longitudinal SEP electrophysiology recordings ( $n=8$ ) before and at 1, 2, 3, and 4 weeks after moderate brain injury. Pre-injury data served as control data. In addition, to control for any effects of experimental conditions on BOLD or SEP data, we first acquired data by stimulating the unaffected limb in order to confirm the expected cortical activation indicating optimal experiment conditions. As a result, low or absent activations elicited by subsequent stimulation of the affected limb could be attributed solely to the effects of injury and not to artifacts of experimental condition. All experimental procedures were approved by the University of California, Los Angeles (UCLA) Institutional Animal Care and Use Committee.

### Brain injury

Adult male Sprague-Dawley rats (320–350 g) purchased from Charles River Breeding Labs (Hollister, CA) were acclimated to standard housing conditions for 1 week prior to use. Throughout the study, rats were allowed access to food and water *ad libitum*. Brain

injury was conducted as described previously by our lab.<sup>17–20</sup> Briefly, following anesthetization with isoflurane (3% induction, 1–1.5% for maintenance) vaporized in oxygen flowing at 0.8 L/min flow rate, the rat was placed in a stereotaxic frame (Stoelting Co., Wood Dale, IL) and the scalp was shaved. Body temperature was maintained throughout the surgery using a thermostatically-controlled heating pad. After cleaning the scalp with alternating betadine and ethanol scrubs, 0.1 mL of the local anesthetic bupivacaine was injected subcutaneously at the midline of the scalp before the skull was exposed via a midline incision.

A 6 mm diameter craniotomy was created using a dental drill with intermittent perfusion with sterile saline to prevent heating. A surgical microscope was used to expose the left hemispheric sensorimotor cortex 0 mm from bregma and –2.5 mm lateral from the midline. Injury was induced by controlled cortical impact (CCI) whereby a 3 mm  $\emptyset$  flat tip was advanced through the craniotomy tangentially onto the dural surface at 20 psi (1.3 m/sec;  $n=7$ ) or 30 psi (1.8 m/sec;  $n=4$ ) to a depth 2 mm below the dural surface with a 250 msec dwell time, resulting in a left-side injury focused over the primary sensorimotor cortex. Two speeds were used to induce mild-to-moderate injury in order to try to reproduce real-world variation in clinical injuries that are used in research studies. Injury severity was assessed in an unbiased automated fashion using quantitative brain atrophy measures (see below), which resulted in final subgroup assignments of five mild and six injured rats. An image was acquired through the microscope for all injuries for later verification of the presence of a subdural hematoma. The craniotomy was then sealed with a layer of non-bioreactive, Kwik-Cast silicon elastomer (Sarasota, FL) and the scalp was resutured and covered with a layer of bupivacaine local anesthetic solution and triple antibiotic ointment. Animals were placed in a recovery chamber with ambient temperature maintained at  $\sim 28^{\circ}\text{C}$  until they had awoken from anesthesia and then returned to their home cages. No mortalities occurred due to acute post-traumatic complications.

### MRI

A 7 Tesla Bruker MR spectrometer running Paravision 5.1 (Bruker, Billerica, MA) was used to acquire structural and functional data before and at weekly intervals after brain injury. Rats were briefly anesthetized with 4% isoflurane in oxygen flowing at 0.6 L/min in order to administer medetomidine sedation (0.05 mg/kg in sterile saline)<sup>21</sup> via the penile vein. Following placement of a subcutaneous cannula and initiation of continuous infusion of medetomidine (0.1 mg/kg/h), the rat was transferred to a purpose-built cradle and secured using 3-point immobilization of the head with two ear bars and a tooth bar. Respiration was monitored remotely and temperature was homeothermic-controlled by forced air (SA11 Instr, Inc.). The S116 Bruker gradients (400 mT/m) were used in combination with a birdcage transmit and an actively decoupled receive-only surface coil to acquire the data. Following a multi-slice gradient echo pilot scan to optimize positioning within the magnet, localized shimming was performed on the head to improve B0 homogeneity.

**fMRI.** A multi-slice, gradient-echo, single shot echo-planar imaging sequence (repetition time (TR)=2 sec, echo time (TE)=30 msec, no averages and using  $14 \times 0.75$  mm thick coronal, slices with a  $30 \text{ mm}^2$  field of view and a data matrix of 128 read by 64 phase-encoding steps) was used to acquire BOLD data during repeated electrical stimulations (10 Hz, 3.5 mA) of affected and unaffected forelimbs in separate experiments that each used an “off-on-off” block design repeated thrice, with each block consisting of 60 sec off, 40 sec on, and 60 sec off. Limb stimulation was evoked through a pair of steel electrodes positioned subcutaneously while the rat was under the initial period of isoflurane anesthesia through the thenar and hypothenar pads on each paw, so that the electrode tips lay just distal to digit numbers 2 and 5, under pads 1 and 3, respectively.

fMRI data acquisition began at 20–30 min after the termination of the initial 10-min period of isoflurane anesthesia. After two runs of stimulus-evoked fMRI acquisition, isoflurane anesthesia was reinstated and detomidine infusion was discontinued.

**Structural.** A two-dimensional rapid acquisition with relaxation enhancement (RARE) sequence was used to collect T2-weighted images with TR = 6018 msec, TE = 56 msec, and RARE factor = 8, and using the same geometry as used for the fMRI protocol, except a data matrix of 128-read by 128-phase encoding steps. At the end of the imaging session, sedation was reversed using antisedan (1.0 mg/kg, intraperitoneally). Rats recovered to the awake state and resumed exploratory behavior in their home cages within 2 minutes of this reversal injection.

### Image analysis

**fMRI.** Data were weighted Fourier transformed to  $128 \times 128$  and converted to compressed Neuroimaging Informatics Technology Initiative format for entrance into the FEAT analysis pipeline.<sup>22,23</sup> First-level analyses were run after brain extraction, motion and slice timing correction, 5 mm spatial smoothing, and a high-pass filter (100 sec). Data were analyzed using the general linear model by fitting a hemodynamic response function composed of a square wave according to the stimulus protocol timing, convolved with a single gamma variate function to derive the temporal derivative waveform. Analysis was performed using temporal filtering and using FMRIB's improved linear modeling with pre-whitening while including motion correction parameters in the model. Data were co-registered to a study-specific anatomical template using FLIRT<sup>24</sup> with 12 degrees of freedom and a cost function. Statistical maps were initially cluster thresholded at  $z = 1.7$  and  $p < 0.05$  based upon pre-injury data showing the expected robust activation within the sensory-motor cortex. Higher level group analyses were run between baseline and post-injury data using FMRIB's local analysis of mixed effects<sup>25</sup> with automatic outlier de-weighting and with contrasts cluster thresholded at  $z = 1.7$  and  $p < 0.001$ .<sup>26,27</sup> Initially, the T2-weighted images were used for segmentation of the contused from non-contused tissue using manual tracing based on the well-defined border of hyperintensity at 4 weeks post-injury. These were displayed as an overlap map after warping the data to a common template space using the transformation parameters obtained from the fMRI analysis. A more objective gray matter volume analysis was also conducted via tensor-based morphometry (TBM; see below) from the T2-weighted anatomical data at 4 weeks after injury and were used as a surrogate measure of injury severity for the fMRI analysis. These data were used as a covariate of interest to determine whether brain activation was modulated by the severity of the ipsilateral injury.

### TBM

TBM was used to measure local volumetric differences on T2-weighted structural data pre-injury and at 4 weeks post-injury as an indicator of injury severity, implemented in a similar manner as before<sup>28,29</sup> with the LONI pipeline.<sup>30</sup> Earlier post-injury structural data were not analyzed in the same way because temporary, acute time-point edema would confound the loss of brain tissue in a developing contusion. Briefly, following brain extraction of pre-injury and 4-week data with BET2,<sup>23</sup> data were corrected for B1 field intensity correction using the nonparametric, non-uniform intensity normalization N4 algorithm.<sup>31</sup> A minimum deformation target (MDT) image was created by aligning all subject volumes to all other volumes using a mutual information-based, inverse-consistent algorithm, followed by applying the inverse of the mean displacement field from all subjects to the MDT.

Next, image volumes in subject space were aligned to the MDT by nonlinearly deforming the anatomy of each image to the MDT, while optimizing the regularity of the deformation by quantifying

the inverse consistent symmetric Kullback-Leibler distance between the MDT and the resulting deformation to allow for unbiased registration.<sup>28</sup> The Jacobian matrices were derived from the displacement field calculated from each image-to-MDT template co-registration. The Jacobian determinant of the matrix is a univariate measure that represents the fractional volume change required to match the template image to each subject space, and represents relative tissue volume differences between each rat and the MDT. A gray matter region of interest was drawn on the MDT within the area encompassed by injury in all rats. Regions were warped to subject space to obtain mean gray matter Jacobian values for each rat as a surrogate for severity. Unsupervised k-means clustering (Matlab, 2011a; Mathworks) was used to classify individual values into different injury level subgroups. Correlation analysis of TBM values and activated voxel counts were conducted by Spearman's rank correlation.

**Immunohistochemistry.** c-FOS immunohistochemistry data were obtained using a previously published method<sup>18</sup> from eight rats used for MRI together with an additional seven injured rats at 5 weeks after injury (CCI; 20 psi, 1.4 m/sec). Briefly, rats were continuously stimulated by electrical stimulation of the unaffected forelimb for 1 h while under medetomidine anesthesia as for fMRI, following which they were kept in a quiet environment for a further 2 h. Following terminal barbiturate anesthesia, they were transcardially perfused-fixed with saline and 4% paraformaldehyde, the brains were cryoprotected, sectioned at  $50 \mu$ , incubated with goat anti-c-FOS primary antibody (#PC38; Calbiochem, San Diego, CA; 1:200), which was amplified using biotinylated secondary antibody (Vector Laboratories, Burlingame, CA; 1:500) and visualized using the diaminobenzidine reaction product. Eight mounted sections,  $650 \mu$ m apart were used to measure cortical gray matter (GM) volume/hemisphere and expressed as loss of ipsilateral cortical gray matter (ipsilateral GM – contralateral GM/contralateral GM  $\times 100$ ) using Stereoinvestigator software (MicroBrightfield Inc., Williston, VT). Unsupervised k-means clustering (Matlab, 2011a; Mathworks) was used to classify the GM loss data into the smallest number of groups based on the data through minimizing the variance within each group and maximizing it between groups. This resulted in two groups, which we operationally defined as mild and moderate injury severity, merely as indicated by the difference in loss of GM tissue, and not in reference to any type of standard severity level across the TBI field. The original eight rats were clustered into a mildly injured ( $n = 4$ ) group and a moderately injured ( $n = 4$ ) group, the same designation as for fMRI and an additional seven rats were classified as six mildly injured rats and one moderately injured rat. One mildly injured rat did not produce high quality c-FOS staining and therefore it was removed so that the total group size was nine mildly injured and five moderately injured rats.

Three sections/brain,  $650 \mu$ m apart, were used to compute c-FOS density bilaterally within gray and white matter regions using Stereoinvestigator software (MicroBrightField, Inc, Williston, VT) interfaced to an M2 upright microscope (Zeiss, Thornwood, NY). Group versus region cell density data were tested for mild versus moderate injury differences using linear mixed effects models with Dunnett's *post hoc* multiple comparison for correction of multiple regions using a one-tailed test (R, version 3.13, packages lme, multcomp).<sup>32</sup> A one-tailed test was implemented since the *a priori* hypothesis generated from the fMRI data was that an increase in c-FOS density would be found in moderately injured rats compared with mildly injured rats.

### Sensory-evoked cortical recordings

A parallel series of eight injured rats (CCI 30 psi, 1.8 m/sec) was used to investigate the cortical sensory evoked potential before and after injury. Two electrode montages were used to cover the extent of the contralesional cortex. Montage A ( $n = 4$ ) consisted of three

stainless steel epidural screw electrodes of  $\varnothing = 1.19$  mm (including threading) over the anterior aspect of the forelimb sensorimotor cortex (SMC) at coordinates relative to bregma: (2.0, 2.0 mm), (1.5, -1.0 mm), and (4.0, -1.0 mm). Montage B ( $n = 4$ ) consisted of five electrodes that overlapped with Montage A, with electrodes placed at: (3.0, 2.0 mm), (2.0, 0.0 mm), (4.5, 0.0 mm), (2.0, -2.0 mm), and (4.5, -2.0 mm). A reference electrode was placed midline in the frontal bone. A hand drill (model DH-1 holder, D#60 bit; Plastics 1, Roanoke, VA) set to 0.8 mm depth and diameter of 1.00 mm was used to fine tune the depth and width of the smaller pilot hole so that recording electrode screws could be set into the skull with 1/2 turn or less. These precautions ensured that the dura was not deformed at any time throughout the drilling or electrode placement procedure. Insulated electrode leads were connected to gold-plated sockets within a plastic pedestal and dental acrylic was used to anchor it to the skull over the electrodes. The location of the skull that would later be removed for CCI injury was covered with silicon elastomer (WP Inst, Sarasota, FL) and a thin layer of dental acrylic for easy removal. Each montage was implanted one week prior to control recordings and 2 weeks in advance of CCI injury.

SEPs were recorded using the MP150 Biopac system (Biopac Systems, Inc., Goleta, CA). Single and paired-pulse SEPs (PP-SEPs) were recorded over the contralesional cortex evoked by 2.0 mA electrical stimulation of the unaffected forelimb using bipolar, 1 msec square pulses, and while under the same medetomidine sedation as detailed before for the MRI study. The inter-stimulus interval (ISI) between pulses was varied between 30, 35, 40, 50, 100, and 200 msec. One week after the pre-injury PP-SEP recording, rats were anesthetized with isoflurane and the left side of the electrode headset was removed with a dental drill and CCI was performed through the left side of the headset as described above. The contused cortex and craniotomy was sealed with a thin layer of silicon elastomer and the headset was re-closed with dental acrylic. Further PP-SEP data was acquired at 3 days and 1, 2, 3, and 4 weeks post-injury.

### SEP analysis

The first 23 of 35 acquired time-locked PP-SEP epochs of 350 msec duration were averaged offline using the ensemble averaging function within the Acknowledge Software v4.1.1 (BioPac Systems, Inc., Goleta, CA). Peak amplitudes of the evoked response (N1) were measured from the baseline immediately following the first (stimulus A) and second (stimulus B) stimulus artifacts for N1A and N1B for each ISI at each time-point. The PP ratio was calculated as the ratio of the second response amplitude relative to the first (N1B/N1A) as a function ISI time. Data were averaged over all electrode pairs (three or five electrodes, Montage A and B, respectively) within each rat, and final data were obtained by averaging across all rats ( $n = 8$ ). Peak latency, amplitude, and peak ratio data are shown as normalized to pre-injury values, and this was achieved on a per electrode, per rat basis prior to averaging within each rat over all electrode pairs, and then finally across all rats. Group univariate statistics were analyzed as peak latency and peak ratio raw data values compared with pre-injury using linear mixed effects analysis of variance (r version 3.3.2, LME function from the NMLE package) with Dunnett's *post hoc* multiple comparison correction for multiple time-points. A one-tailed test was used based on the *a priori* hypothesis arising from the BOLD data that increased excitability was anticipated at post-injury time-points.

## Results

We operationally define the hemisphere opposite the left, primary injured hemisphere as "contralesional," and the injured hemisphere as "ipsilesional." This is done in preference to using contralateral and ipsilateral, which do not accurately reflect the intended regional focus of the text when describing hemisphere-specific brain acti-

vation in response to stimulation of left or right forelimbs. In regard to limb nomenclature, we refer to the right limb, which is predominantly affected by injury and which lies opposite the ipsilesional hemisphere, as the "injury-affected limb." We refer to the right limb that is opposite the contralesional hemisphere, and which is less affected by injury, as the "unaffected limb."

### *Transient ipsilesional-to-contralesional shift of the injury-affected forelimb cortical representation followed by reduced ipsilesional map chronically*

To determine how the cortical map that governs affected forelimb control changes throughout recovery after TBI, affected forelimb-evoked fMRI data were acquired from 11 adult rats before and at weekly intervals following either mild or moderate CCI injury of the left primary sensorimotor forelimb (S1-FL) cortex. These data show that CCI brain injury initiated a trans-hemispheric shift in the group-averaged, affected forelimb-evoked BOLD activation from the injured to the opposite contralesional cortex over the first week of recovery (Fig. 1A-C; overall mean group effect  $p < 0.001$ ). This was readily apparent in seven of 11 rats at 1 week, while there was a total absence of activation anywhere in the remaining four rats that survived statistical thresholding (individual data points not shown). We confirmed that the absence of this activation did not occur due to insensitivity to the BOLD response arising from experimental conditions, because we observed brain activation elicited by the unaffected limb in all case. At 2 weeks post-injury, the activation pattern was wide-spread and bilateral (11 of 11 rats) covering a large region of the contralesional cortical hemisphere, even while ipsilesional areas surrounding the injury site also were activated. However, over the subsequent weeks of recovery, the mean activation map shifted back to the opposite, contralesional S1-FL cortex (seven of 11 rats at 21 days), then remained largely subcortical in 10 of 11 rats at 28 days (overall mean group effect  $p < 0.001$ ).

Given the within-group variation post-injury, it was not surprising that direct statistical comparison of these activation patterns to the pre-injury data using voxel-wise analyses did not show any differences that survived the multiple-voxel cluster correction ( $p > 0.001$ ). Similarly, voxel counts of activated voxels at the subject level revealed that the volume of activated cortex within the contralesional cortex also did not reach significance compared with pre-injury (Fig. 1B), although removing four of 11 rats at 1 week post-injury that did not activate at all did result in a significant difference (not shown,  $p < 0.05$ ). Despite this however, the number of activated voxels within the injured hemisphere decreased to approximately half of pre-injury values over the first 2 weeks following injury, then again at both 3 and 4 weeks, to approximately 10% of the pre-injury volume ( $p < 0.05$ ; Fig. 1C). This occurred despite the steady resumption of more normal limb-reaching previously reported in this TBI model in an independent study.<sup>33</sup> These data indicate that regions of the brain other than the injured cortex may be responsible for spontaneous resumption of limb function over the first month of recovery, and that the contralesional hemisphere may support this, but only early and not later after injury.

### *Transhemispheric shift is injury severity-dependent at 1 week post-injury*

We next investigated whether differences in injury severity accounted for the within-group variations in activation volume. Initial assessment of injury by manual contusion volume measurements using the T2- anatomical images acquired at 4 weeks post-injury

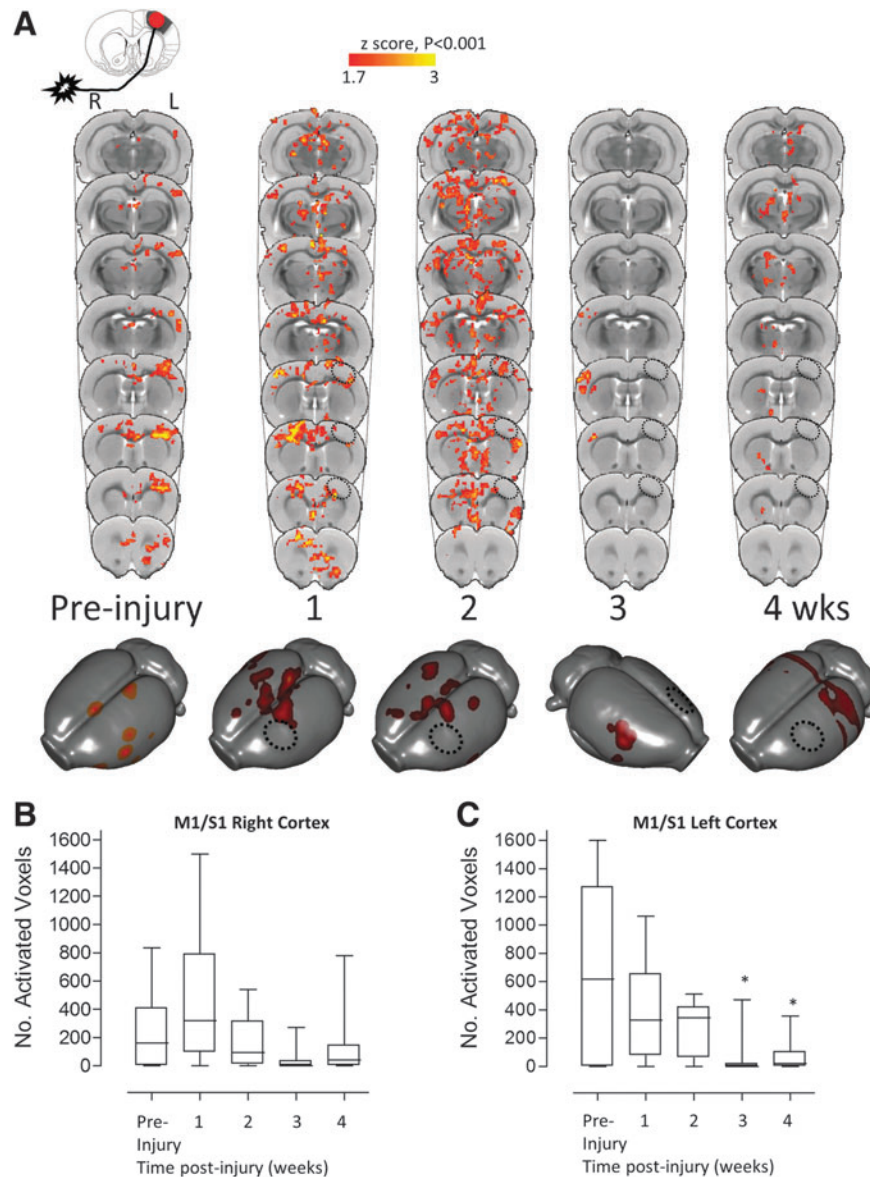


**FIG. 1.** Deficits in injury-ipsilateral forelimb circuitry are revealed by affected forelimb-evoked brain activation by blood oxygenation level-dependent (BOLD) functional magnetic resonance imaging (fMRI). **(A)** Group mean, affected (right) forelimb-evoked activation data (one-tailed  $t$ -test, corrected for multiple comparisons,  $p < 0.001$ ,  $z > 1.7$ ) before and at 1, 2, 3, and 4 weeks after injury, superimposed on a rat brain template as coronal image plots and surface-warped data. Plots of **(B)** number of significantly activated voxels in the right M1 and S1-forelimb cortex contralateral to the stimulated limb (ipsilateral to the injury site) and **(C)** number of activated voxels in the cortex ipsilateral to the stimulated limb (contralateral to the injury site). Data show widespread injury-ipsilateral inactivation after injury (A) that was significant for time in the injury-ipsilateral (left) M1/S1-forelimb cortex (C,  $p < 0.001$ ) and specifically at 3–4 weeks post-injury (C,  $*p < 0.05$ ). Data also show that there were early diffuse activated regions contralateral to the injury, ipsilateral to the stimulated limb (A) that was variable between rats because the mean effect was not significant for the number of activated voxels in contralateral (right) M1/S1-forelimb cortex (B). Key: Hatched circle represents approximate position of primary injured region.

revealed a range of cortical damage (Fig. 2A). Injury severity was then more formally determined by TBM in the same images to obtain an estimate of gray matter atrophy (Fig. 2B). This unbiased technique is based on minimizing the within subgroup variance and maximizing the between subgroup variance in the data (see Methods). Using unsupervised k-means clustering, two separate groups emerged characterized by mild and moderate injury ( $-1.0$  and  $+23.8\%$  change in volume,  $n = 6$  and  $5$ , respectively). Subsequent voxel-wise analysis of BOLD activation volume based on these differences in injury severity revealed a severity-dependent increase

in activation in both peri-contusional and contralesional white and gray matter regions at 1 week post-injury (Fig. 2C). Further, the volume of contralesional BOLD activation assessed by counts of activated voxels in each subject at 1 week post-injury was significantly correlated with the degree of ipsilesional cortical gray matter damage reported by TBM at 4 weeks post-injury ( $R^2 = 0.65$ ,  $p < 0.05$ , two-tailed; Fig. 2D) as well as with more ipsilateral activation ( $R^2 = 0.77$ ,  $p < 0.01$ ), but not at later time-points (not shown). In other words, greater damage to the ipsilesional cortex resulted in an initial broad, bilateral activation acutely, but this correlation did

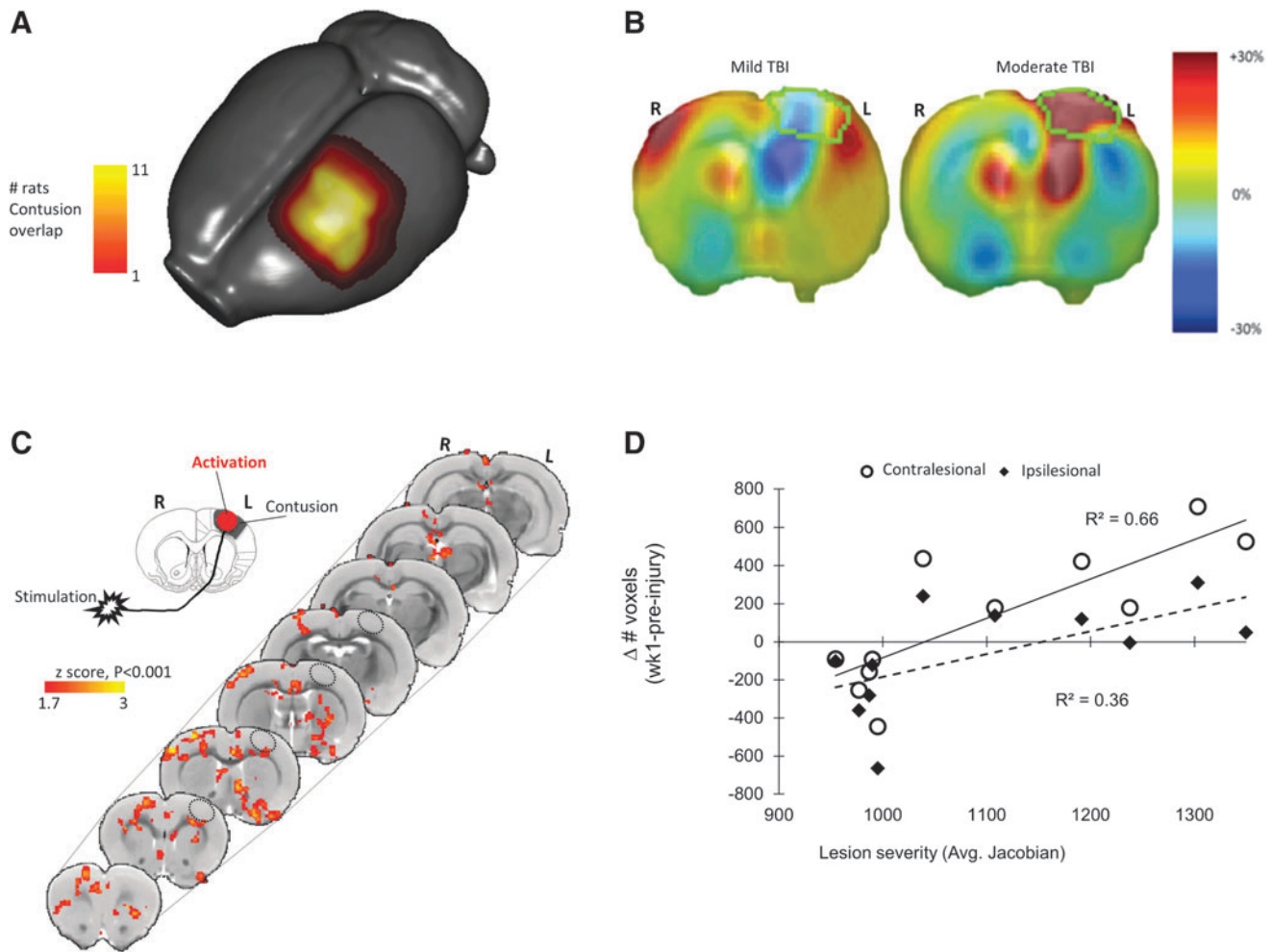


**FIG. 2.** Greater injury is associated with a greater shift in cortical activation to the contralesional (right) hemisphere in response to affected (right) forelimb-evoked activation at 1 week post-injury. **(A)** Stacked, surface projection plot of contusion volume masked from the T2-weighted structural image of each rat at 4 weeks post-injury and warped into template space. Data shows that there are a range of injury severities within the group indicate by the presence of contusion in 11 rats (yellow region) but extending further out in only 1-5 rats (red regions). **(B)** Representative Jacobian maps of the same data confirming different degrees of brain injury at 4 weeks consistent with mild-to-moderate levels of brain injury (outlined region indicates the region drawn in mean deformation target image space used to obtain average Jacobian values in subject space). **(C)** Group-level, statistical contrast maps of affected forelimb-evoked brain activation differences between mild and moderate injured rats at 1 week post-injury (mean cortical Jacobian percentage values  $0.7 \pm 1.9$  versus  $23.8 \pm 3.5\%$ , respectively from (B) showing regions where moderate > mild group brain activation). Data show a greater left-to-right shift in the degree of cortical activation in response to affected forelimb stimulation after moderate compared with mild injury, two-tailed  $t$ -test,  $n = 6$  vs. 5, respectively;  $z = 1.7$ ,  $p < 0.001$ . **(D)** A linear regression analysis plot of number of activated voxels/rat in contralesional (open circles, solid line) and ipsilesional cortex (closed diamonds, dashed line) at 1 week post-injury versus injury severity (average gray matter Jacobian raw value) at 4 weeks. Data show a significantly greater contralesional (right) activation response in moderately injured rats (solid line,  $R^2 = 0.65$ ,  $p < 0.05$ ), as well as more ipsilateral activation (Dashed line,  $R^2 = 0.77$ ,  $p < 0.01$ ). Activation data after 1 week post-injury were not significantly correlated with severity (not shown). Key: Hatched circle represents approximate position of primary injured region.

not persist at later post-injury time-points as the contralesional cortex became dominant in activation (see next section).

#### *Unaffected forelimb-evoked contralesional BOLD signal increases at 4 weeks post-injury*

Based on a working hypothesis that remote excitability changes would occur after brain injury, perhaps in a similar manner to stroke,<sup>34</sup> and from evidence from functional and structural connectivity changes in the CCI model,<sup>17,20</sup> we investigated changes in the less affected, contralesional hemisphere for activation changes

under control of the unaffected forelimb in the same cohort of rats. As expected, the focus of the pre-injury group mean activation evoked by stimulation of the unaffected limb was contralesional, unilateral, and centered on the sensory S1FL, with some overlap to cortical motor regions (Fig. 3A). While some degree of broadening of the activation occurred at 1 week post-injury with subsequent refocusing at later times, no voxel survived the multiple comparison correction, although it was just outside of significance at 4 weeks ( $p > 0.001$ ). We pursued this preliminary trend and quantified the BOLD signal change at subject level, but constrained to brain regions within the mean group activation masks. For each



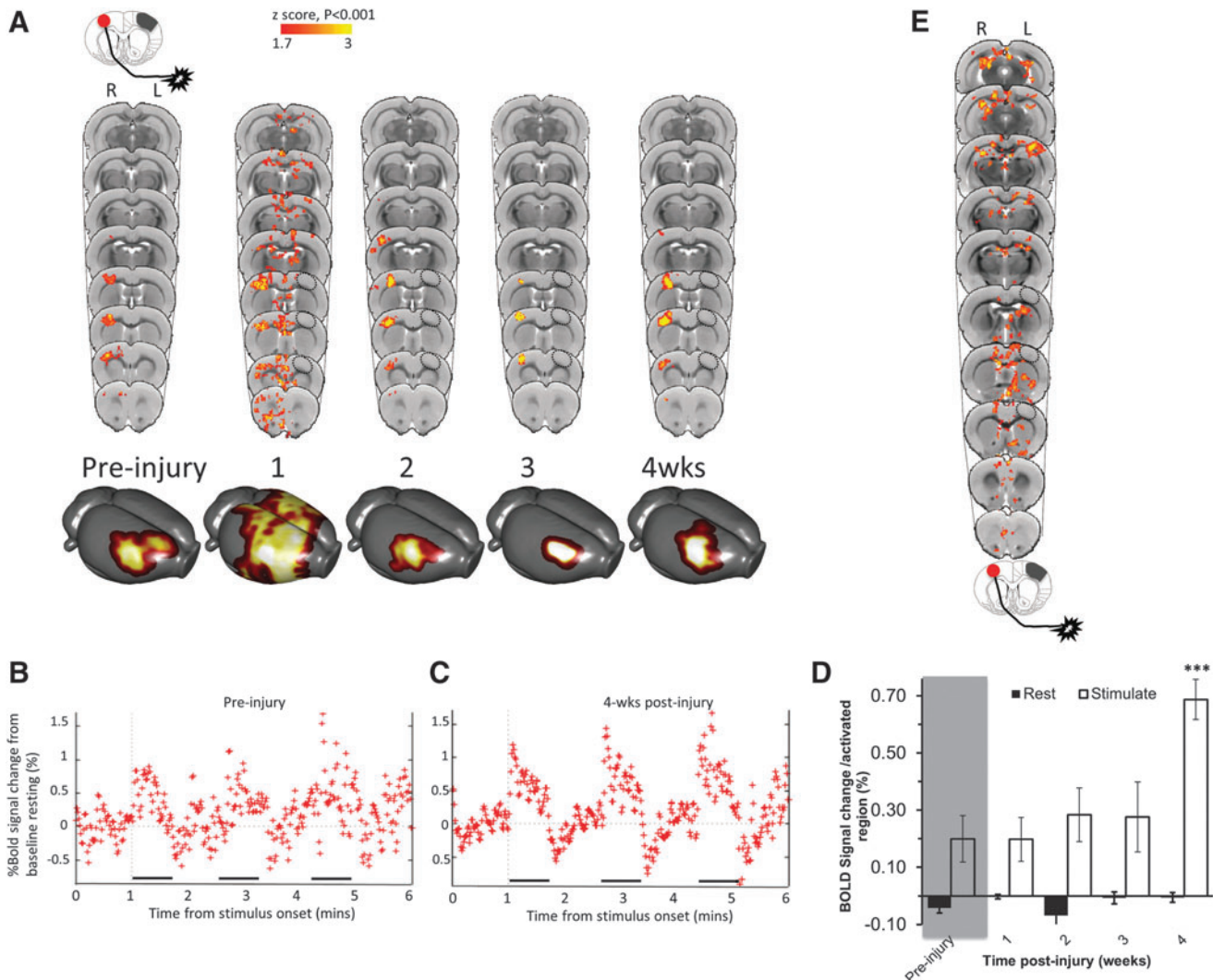


**FIG. 3.** The degree of contralesional blood oxygenation level–dependent (BOLD) activity increases at 4 weeks in response to unaffected limb stimulation. **(A)** Group mean, unaffected (left) forelimb–evoked activation data (one-tailed  $t$ -test, corrected for multiple comparisons,  $p < 0.001$ ,  $z > 1.7$ ) before and at 1, 2, 3, and 4 weeks after injury, superimposed on a rat brain template, and also shown as 3D surface projections. **(B, C)** Plots of contralesional cortex BOLD signal percent change during unaffected limb stimulation compared with at rest for all rats imaged **(B)** pre-injury and **(C)** at 4 weeks post-injury. **(D)** Quantified BOLD signal was significantly increased at 4 weeks post-injury compared with pre-injury, but not at earlier time-points ( $p < 0.001$ , linear mixed models analysis of variance). **(E)** Contrast plots of activated gray and white matter brain regions that were positively correlated to injury severity (tensor-based morphometry data) during unaffected forelimb stimulation at 4 weeks post-injury.  $*p < 0.05$ . Key: Hatched circle represents approximate position of primary injured region.

time-point, the statistical mask (Fig. 3A) was back-projected on to the corresponding data-sets in native space in order to obtain average BOLD signal change during forelimb stimulation. BOLD signal changes remained similar to pre-injury until 4 weeks post-injury (Fig. 3B, 3C) when there was a significant increase compared with pre-injury ( $p < 0.001$ , Fig. 3D).

#### *Increase in unaffected forelimb-evoked contralesional BOLD signal is severity dependent*

Given the variability in injury severity found in these rats (Fig. 2B), we investigated whether the contralesional increase in BOLD signal at 4 weeks elicited by stimulation of the unaffected limb also was dependent on the degree of structural damage. We used the TBM data as a covariate of interest in a general linear

model analysis of the BOLD data to determine whether injury severity was associated with changes in BOLD activation. We found that brain activation evoked by unaffected limb stimulation was positively correlated to the severity of injury, not only in the expected gray matter regions of contralesional M1/S1FL cortex, but also in ipsilesional M1 and posterior S1 cortex, and subcortically in caudate internal capsule and thalamic and brain stem nuclei (Fig. 3E). There also were notable bilateral regions of white matter activation that were positively correlated to injury severity (Fig. 3E). We attempted to confirm these findings by analyzing brain sections immunostained for the immediate early gene product c-FOS from a subset of the same rats, as well as additional rats, but after 1 h constant stimulation of the unaffected limb at 5 weeks post-injury. We analyzed gray matter tissue loss and grouped data using unbiased k-means clustering into mild and moderately injured rats based

on low or high tissue loss (Fig. 4C). Representative raw c-FOS+ cell density projections from a subset of eight mildly or moderately injured rats (Fig. 4A, 4B) showed bilateral gray matter activation, similar to that obtained previously with this technique and in this injury model, albeit from affected forelimb stimulation,<sup>18</sup> rather than the current unaffected limb stimulation. Unlike the fMRI, there were only trends towards increases in gray matter c-FOS density in moderately injured unaffected forelimb-stimulated rats compared with mild. However, more consistent with the fMRI findings (Fig. 3E), there were large and significant bilateral increases in white matter c-FOS cell density (Fig. 4B) in moderate versus mildly injured rats ( $p < 0.01$ ; Fig. 4D).

#### Electrophysiologic evidence of increased contralesional excitability

Given the likely contribution of glial cells to the BOLD signal<sup>35</sup> and that gliosis occurs bilaterally after contusion injury,<sup>36</sup> we then sought to determine the direct neuronal responses of the contralesional cortex to forelimb stimulation in a parallel group of eight

moderately injured rats by recording SEPs from the unaffected limb to a grid of screw electrodes on the contralesional skull surface (Fig. 5A). Quantification of the amplitude and latency time to arrive of the first major SEP peak in the cortex (Fig. 5B) revealed no difference in amplitude (Fig. 5D) but a significantly reduced latency time-to-peak, compared with pre-injury, at all post-injury times when averaged over all electrode positions and for all rats tested, suggesting increased cortical excitability (Fig. 5C). To investigate this phenomenon more explicitly, we conducted a PP-SEP experiment (Fig. 6A) with the idea that if a second sensory stimulation was given sufficiently close to the first, then the second SEP would be greater in size after injury, compared with pre-injury, if the cortex was more excitable (Fig. 6B). As expected, PP suppression of the second pulse (shown as a ratio of the paired peaks – PP ratio) among all data regardless of pre- or post-injury time was most pronounced at the shortest, 35 msec inter-stimulus interval (ISI) pre-injury, and diminished as the ISI was extended to 200 msec (Fig. 6C). After injury, we found that among PP ratio data

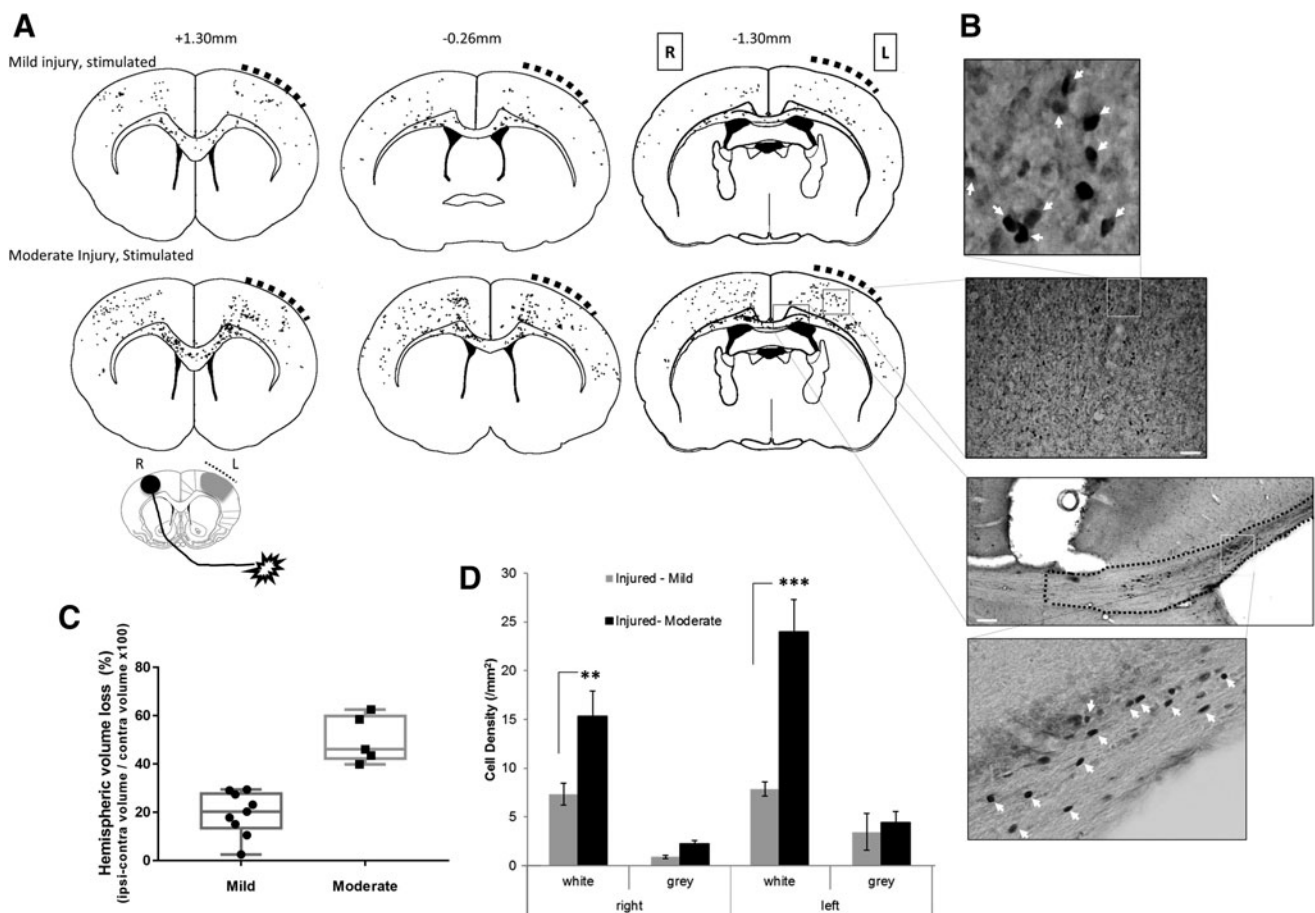


**FIG. 4.** Bilateral white matter activation is greater after moderate compared with mild injury. (A) Co-registered group-wise plots of individual, raw c-FOS+ cell positions after left-side brain injury (bold, hashed curve) after stimulation of the unaffected forelimb. Raw cell data counts are taken from three rats/group representative of mild and moderately injured rats and are overlaid onto an atlas at +1.3, -0.26, and -1.30 mm bregma, for semi-quantitative visual comparison. (B) Representative image of c-FOS+ staining from the cortical gray and white matter together with high-powered insets showing examples of c-FOS+ cells counted (white arrowheads). (C) Plot of percent hemispheric gray matter loss showing the group delineation achieved by k-means clustering of values that were assigned as mild and moderate injury and used for c-FOS group analysis in plots (A) and (D). (D) Plot of c-FOS+ cell density for gray and white matter (corpus callosum) regions for left and right hemispheres averaged from the three brain antero-posterior levels shown in (A), from mildly ( $n=5$ ) and moderately injured rats ( $n=9$ ) at 5 weeks post-traumatic brain injury showing significant difference within white matter regions (linear mixed models, Tukey's *post hoc* corrected,  $***p < 0.001$ ,  $**p < 0.01$ ). Key: L-left, R-right. Scale bar 200  $\mu\text{m}$ .



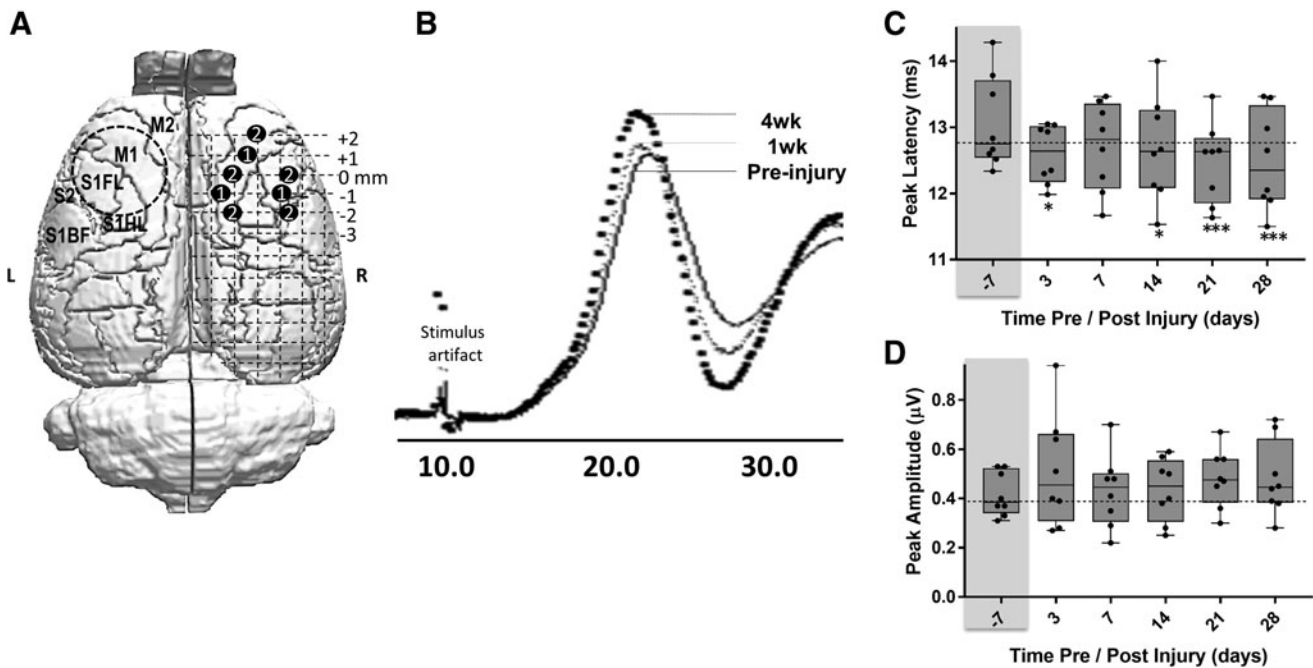


**FIG. 5.** Unaffected forelimb-evoked sensory-evoked potentials in contralesional cortex are reduced in peak latency. **(A)** Stylized figure showing the position of the two electrode designs used in the experiments (labels 1 and 2) in the contralesional right (R) cortex relative to the position of the left (L) hemisphere primary injury site (circular, dashed line). **(B)** Group-averaged sensory evoked potential signal from rats pre-injury (solid line), at 1 week (light gray line) and at 4 weeks post-injury (bolded, dotted line). **(C)** Plot of peak latencies for a single stimulus and response quantified at different times post-injury and showing a significant reduction. \* $p < 0.05$ , \*\*\* $p < 0.001$ . **(D)** Plot of peak amplitudes for a single stimulus showing no significant response at any time-point post-injury.

collected at 100 msec ISI and averaged over all pairs of electrodes pairs (apart from two posterior-positioned pairs that did not respond in the same way, Fig. 7B), the ratio of the peaks was significantly increased compared with pre-injury, but only at 3 days and 4 weeks post-injury, and not between these time-points ( $p < 0.05$ ; Fig. 6C). We found similar albeit nonsignificant trends toward increased PP ratios at short (35 msec) as well as longer (200 msec) ISI times at all post-injury times when averaged over all electrodes (Fig. 6D), further evidence of increased cortical excitability.

To determine if there were any spatial differences in the SEP to identify any particular regions that were more excitable, we plotted mean time-point data for individual electrode pairs at 100 msec ISI, the PP interval resulting in the most robust group differences. The data from the two electrode grid schemes used (white and black numerals, Fig. 7A; dotted and bold lines, Fig. 7B) show some disparity between electrode pairs based on location at 3 days post-injury, as shown diagrammatically (Fig. 7C, 7D). The greatest post-injury PP ratio increase generally occurred between anterior and posterior-positioned electrodes at 3 days post-injury: laterally between the barrel/S1DZ and forelimb cortices, and medially within the M1/M2 cortex. These regions returned to pre-injury levels at 1–3 weeks post-injury but were similarly increased at 4 weeks (Fig. 7C, 7D). Also at 4 weeks, there were increased PP ratio values compared with pre-injury in electrodes located between forelimb and M1 cortex, regions that were initially decreased from pre-injury levels at 3 days post-injury, suggesting some temporal dependence for reorganization in the contralesional cortex.

## Discussion

Although over the last 20 years a plethora of mainly clinical neuroimaging studies have shown that the brain undergoes some

degree of functional as well as structural reorganization after TBI, our understanding of it remains incomplete. The major novel findings in this study contribute to our knowledge in this field by showing that early after injury the affected limb cortical map transiently moves to contralesional cortex, while ipsilesional cortex activation becomes reduced or absent chronically. These latter changes coincide with significant, remote increases in contralesional BOLD and SEP paired-pulse excitability, leading to the possibility that cross-hemisphere changes in excitation prevent more normal ipsilesional evoked activity.

### Ipsilesional hypoactivity—the stunned brain

The prolonged absence of evoked BOLD activity within the ipsilesional, sensory motor cortex is consistent with an absence of ipsilesional hind-limb evoked blood flow changes,<sup>37</sup> an early post-injury abolishment of the SEP,<sup>38</sup> hypoactivity to whisker stimulation in a fluid percussion injury (FPI) model of TBI,<sup>39,40</sup> as well as persistent hypometabolism that persists for up to 2 weeks after CCI injury.<sup>41</sup> On the other hand, the inability of ipsilesional cortical circuits to evoke activity is not entirely consistent with a slice electrophysiology and glutamate biosensor study in adult CCI-injured mice at 2–4 weeks post-injury, where significantly increased ipsilesional glutamate signaling, reduced inhibitory postsynaptic current, and loss of GABAergic interneurons was reported.<sup>42</sup> However, given the wide range of the post-injury time-period studied, the reported heightened network activity does coincide with the unexpected unconstrained activity evoked by affected-forelimb stimulation in the current study at 2 weeks post-injury (Fig. 1A), and with a sudden absence of functional connectivity deficits at the same time in this model.<sup>17</sup> The subsequent prolonged absence of evoked ipsilesional BOLD activity at least until 4 weeks post-injury in the

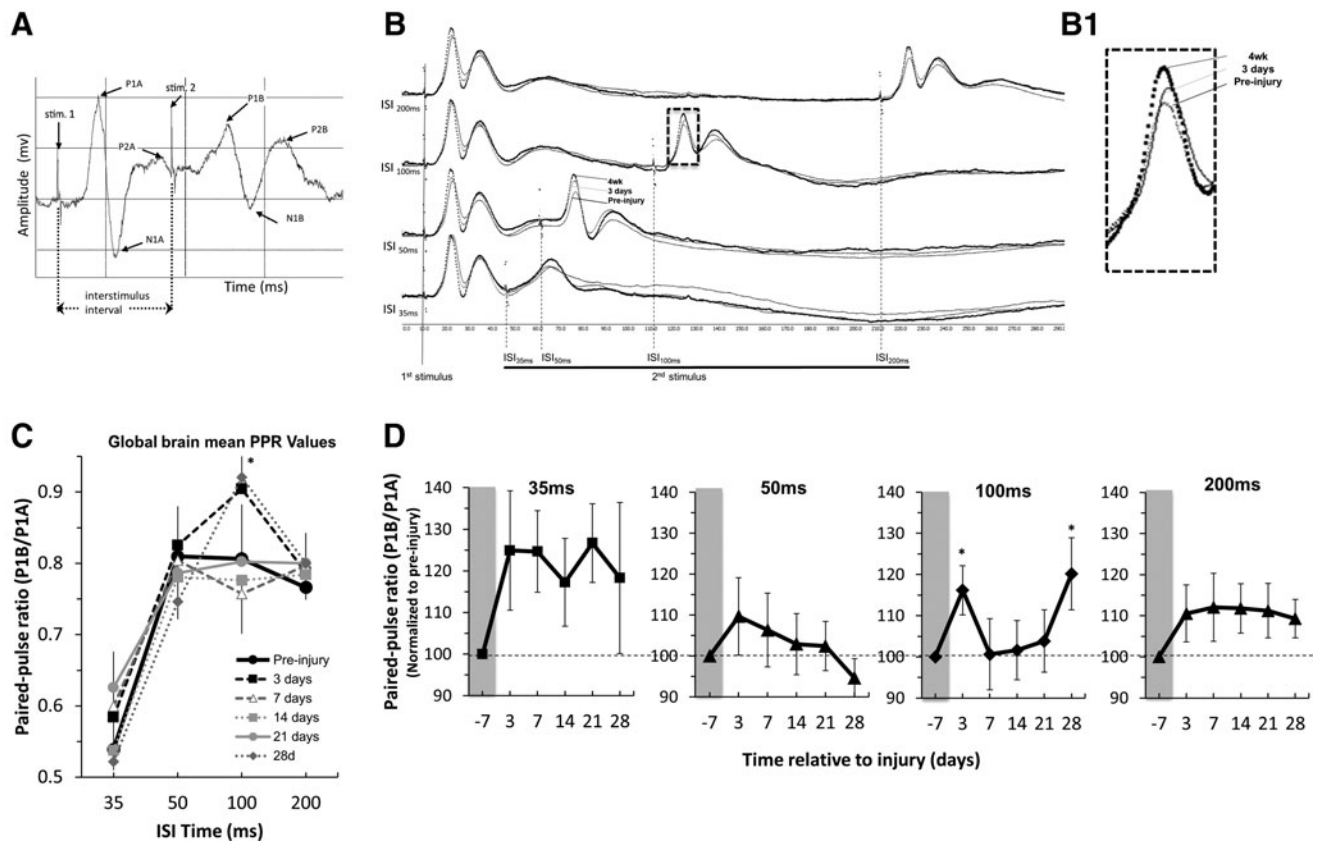


**FIG. 6.** The sensory evoked potential (SEP) paired-pulse (PP) ratio in contralesional cortex is significantly increased at 3 days and 4 weeks after traumatic brain injury. **(A)** An example plot of the paired-pulse design used, showing the stimulus (stim1, stim2), the inter-stimulus interval (ISI) used to delay the onset of the second stimulus, and the resulting SEP pulses (P1, P2, N1) recorded following each stimulus. The pulses immediately following the first and second stimuli (P1A, P1B, respectively) were quantified. **(B)** Group-averaged, SEP signal of the PP stimulus response at 50–200 msec ISI averaged from all electrode pairs, and temporally realigned to the first stimulus artifact to illustrate the lowered second peak amplitude at 100 msec ISI, especially at 4 weeks compared with pre-injury, giving rise to reduced P1B/P1A PP ratios. **(C)** Plot of PP ratio data values from all electrode pairs (apart from two posterior pairs that responded differently; Fig. 7B) and for all post-injury time-points as a functions of ISI time, showing a significant difference at 28 days post-injury at a 100 msec ISI and a trend at 3 days. **(D)** Plots of PP ratio values for each ISI value versus post-injury time and normalized by individual rat pre-injury value. Data shows non-significant trends toward increased PP ratios at 35, 50, and 200 msec ISI at most post-injury times, and a significant increase at 3 and 28 days at 100 msec ISI.  $*p < 0.05$  (Linear mixed models analysis of variance, Dunnett-corrected multiple-comparisons on raw data). Horizontal dotted line = mean pre-injury values.

current study, suggests that data obtained from brain slices may not always closely represent coordinated evoked network activity recorded *in vivo*. In support of the lack of coordinated network activity in the ipsilesional hemisphere after trauma in the current study, prior work after FPI showed that it was still possible to elicit a vibrissae response from the ipsilesional barrel cortex at 1 and 7 days by direct cortical stimulation,<sup>43</sup> indicating that functional deficits occur via altered cortical white matter communication rather than the inability of cells to respond to a stimulus. The continued hypoactivity in the ipsilesional cortex that occurred herein, despite the resumption of more normal reaching patterns by the affected forelimb in sensorimotor tasks by this time,<sup>33</sup> is a clear indication of functional reorganization to other brain regions.

#### *Trans-hemispheric transfer of function and remote changes*

In this study, the degree of cortical hemispheric transfer of function was related to the amount of ipsilateral injury at 1 week, suggesting that the contralesional cortex adopts control of the af-

ected limb, at least acutely. Similar transfer of the cortical map has been shown early after experimental brain injury in the mouse<sup>16</sup> and rat,<sup>15,44</sup> as well as stroke,<sup>45</sup> cortical lesioning,<sup>46</sup> and clinically after stroke.<sup>47</sup> However, the disease mechanisms responsible for altered function after TBI and stroke are likely to be very different given their very different initial causes. Indeed, unlike after stroke, the current data shows that this trans-hemispheric relationship is absent at more chronic times, suggesting that other brain regions controlling forelimb function may become more widely distributed. Indeed, the lack of return of more normal ipsilateral activity controlling this limb chronically that occurs, despite the known spontaneous resumption of behavioral function at this time,<sup>33</sup> suggests that the process of reorganization in this trauma model is both temporally and regionally dependent, and that brain regions in addition to the contralesional cortex reorganize to support affected limb function at longer post-injury times. This also may be related to the severity of the injury because brain lesioning studies have found that the contralesional response of increased synaptogenesis<sup>48</sup> and associated structural changes is muted in rats with larger lesions.<sup>49</sup> Evidence from resting state functional connectivity<sup>17</sup> as

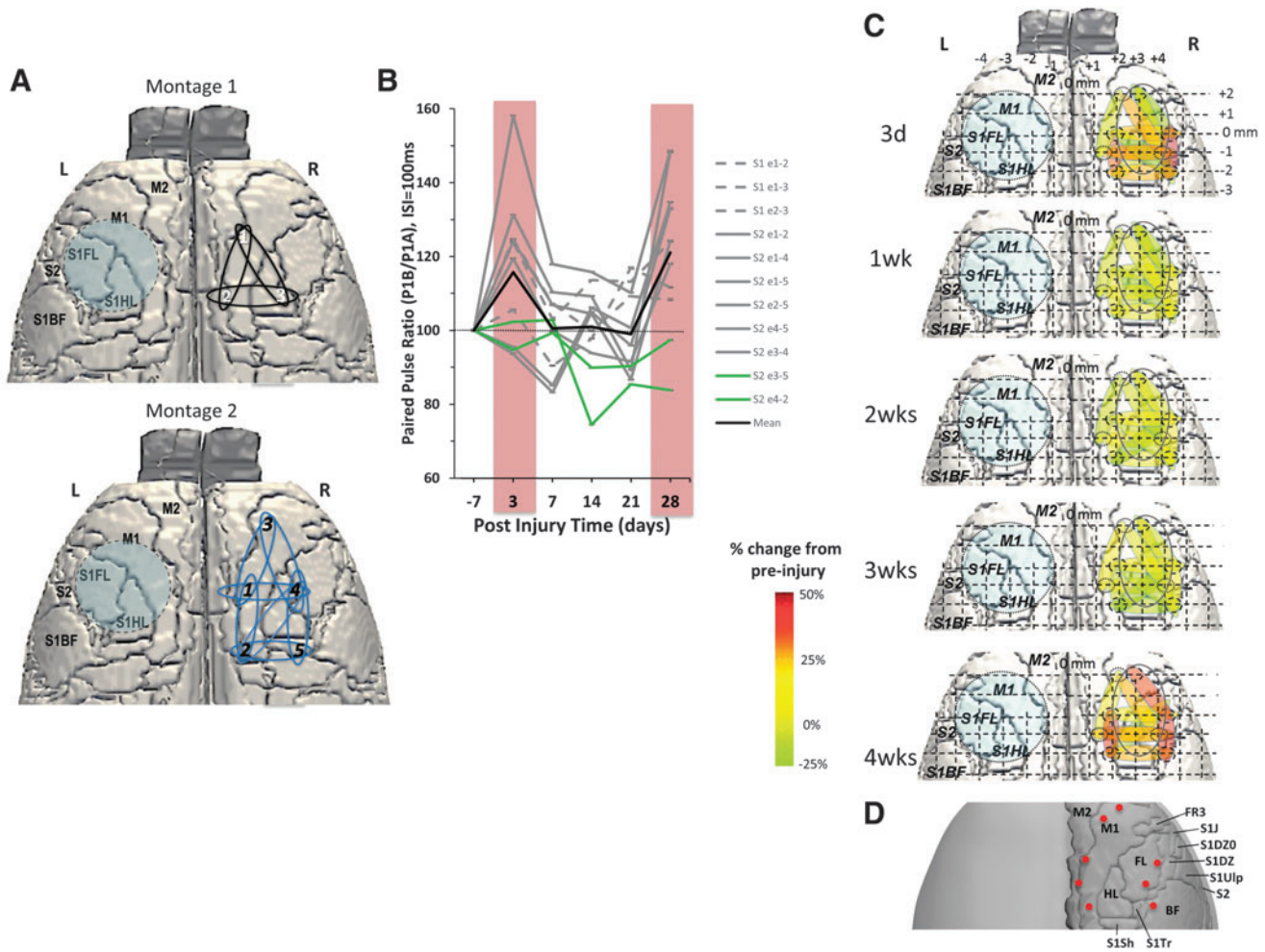


**FIG. 7.** Regional plots of paired-pulse (PP) ratio values at 100 msec indicate acute and chronic time-point pericontusional hyperexcitability. **(A)** Stylized figures showing the position of the two electrode montages used in the experiments in the contralesional (right) cortex, homotopic to the contusion site (blue circle). **(B)** Plot of pre-injury normalized PP ratio values at 100 msec ISI for all electrode pairs averages across rat, and for the two electrode schemes (S1, S2; corresponding to white, black numbers in A, respectively) demonstrating regional differences in the degree of hyperexcitability that contribute to the mean data (black bar) as originally plotted in Figure 5. Two electrode pairs did not respond to the stimulus (green lines, S2-e3-5, S2-e4-2). **(C)** Data in (B) plotted spatially and as a percentage of pre-injury values to demonstrate the robust lateral and posterior increases in PP ratio at 3 days and 4 weeks, but largely normal/pre-injury values intermediate times. **(D)** Summary brain surface atlas superimposed with electrode positions for direct comparisons to data in (C).

well as diffusion tensor imaging data<sup>20</sup> in the same TBI model used herein, does indicate that in addition to early and significant functional and structural disconnection of interhemispheric circuits, there are substantial increases in connectivity that are centered on the contralateral cortex, but that also occur more widely in the brain. The current finding of injury severity–dependent increases in activity within the thalamus and caudate in response to unaffected limb stimulation at 4 weeks (Fig. 3E), and the limitation of brain activity to subcortical regions during affected forelimb stimulation (Fig. 1A) is in agreement with blood-flow autoradiographic data in similar regions in the same model.<sup>44</sup>

The idea that reorganization can occur in subcortical brain regions may make it an important target for neurorehabilitative care using neuromodulatory interventions. On the other hand, regions of reorganization after brain trauma also may be viewed as areas with a connection phenotype at risk for developing seizure type activity. Increased connection probability and efficacy between cortical neurons occurs weeks after trauma using the cortical undercut

model,<sup>50</sup> and data suggest that homeostatic synaptic plasticity compensates for regions of decreased activity leading to uncontrollable cortical hyperexcitability.<sup>51</sup> Therefore, potential neuromodulatory therapies after TBI will likely have a dual role in the brain: to promote activity in hypoactive regions, but also to prevent the longer-term development of hyperconnectivity in spatially distinct but connected brain regions.

*Electrophysiology and BOLD evidence of altered excitation-inhibition*

The latency of the arriving SEP signal in the contralesional cortex was significantly reduced early and persistently after injury, either indicating an increased efficiency of nerve conduction along the neural pathway, or reduced threshold for activity within the cortex, or both. However, changes in SEP latency were not matched by a significant increase in evoked BOLD signal within the contralesional cortex activation focus until 4 weeks post-injury. Since

altered neurovascular coupling is less likely in this injury-remote region, as supported by the similar c-FOS results, at least in white matter, it may indicate that the SEP is a more sensitive indicator of contralesional reorganization than fMRI-evoked BOLD activation. This is likely because data in the same model demonstrated increases in correlated BOLD signal or functional connectivity in the contralesional cortex as early as 1 week post-injury.<sup>17</sup>

In support of increased efficiency of the SEP neural pathway, there is structural evidence of contralateral changes in the corticospinal tract portion of this circuit at least by 4 weeks post-injury, as indicated by altered diffusion tensor imaging indices and increases in fiber tract densities.<sup>20</sup> In fact, reorganization at the level of the corticospinal tract would have far-reaching effects on reorganization of higher brain centers, especially the contralesional cortex. Whether or not remote contralesional reorganization is beneficial for behavioral outcome after TBI in the long term is unknown, since a greater activity-dependent effect from this circuit due to training is maladaptive to the affected limb after a unilateral sensorimotor lesion.<sup>52</sup> That this latter effect was shown to be dependent on an intact connecting corpus callosum is of particular relevance to the present study, where we found significant, bilateral white matter activation when stimulating the unaffected forelimb detected by both fMRI (Fig. 3E) and c-FOS (Fig. 4A), indicating that input from the unaffected limb provokes activity within the ipsilesional circuitry. Whether or not this is a direct neuroimaging readout of a maladaptive response remains to be proven.

The measured increased in PP ratio of the SEP signal at 3 days and 4 weeks post-injury, but not between these times, is somewhat incongruent with the persistent decrease in SEP latency times and suggests that different mechanisms are driving these phenomena. A study measuring PP ratio data after TBI recorded from the hippocampus in slices reported decreases in PP ratio, indicative of increased inhibition,<sup>53</sup> commensurate with the development of aberrant sprouting and seizure activity.<sup>54</sup> Other studies have shown increased hippocampal PP ratio data,<sup>55,56</sup> indicative of a reduction in synaptic inhibition or an increase in excitability. There is no simple relationship between tissue injury, as indicated by biomechanical strain and PP ratio data,<sup>57</sup> and spatial differences in excitability may further complicate the interpretation, at least within hippocampus.<sup>58</sup>

Cortical PP ratio data recorded from brain slices reported transient increases in contralesional cortex excitability at 1–2 days post-injury after CCI injury in the adult rat, which then normalized by 3 days.<sup>16</sup> These *ex vivo* findings are somewhat comparable to the current *in vivo* data whereby early increases in excitability at Day 3 were lost by 1 week. The early post-injury increases in excitability are likely to result from an entirely different mechanism to the later onset of cortical excitability. For example, they may well be linked to the massive net extracellular ionic fluxes and neurotransmitter changes that occur early after injury,<sup>59</sup> which promotes hypermetabolism,<sup>60,61</sup> with later increased frequency of miniature excitatory postsynaptic currents in both axotomized neurons at 1 day and intact neurons at 2 days after injury.<sup>62</sup> A cortical lesion model showed that these early effects are likely to be driven by GABAergic rather than AMPA receptor-mediated events.<sup>46</sup>

There are several potential mechanisms for the increased PP ratio, or PP facilitation (PPF), a form of short-term synaptic plasticity. PPF can occur both at the level of the thalamocortical afferents<sup>63</sup> and directly in the neocortex.<sup>64</sup> PPF is related to accumulation of residual Ca<sup>2+</sup> in the pre-synaptic terminals after the first stimulus, and is generally thought to relate to a lower vesicle release probability from the first pulse<sup>65</sup> so that the second pulse results in a greater response.<sup>63</sup> Pre-synaptic K<sup>+</sup> channel

currents are known to be involved in PPF in the mammalian brain<sup>64</sup> and their long-lasting deficits after FPI have been associated with increased excitability,<sup>65</sup> making them possible candidates responsible for the enhanced PP ratio found in the current data. While the impact of pre-synaptic Ca<sup>2+</sup> concentration on excitability is well known acutely after TBI, there are no data to suggest an involvement at extended times post-injury. However, given the major role of astrocytes in TBI pathology<sup>66</sup> and their controversial role as modulators of synaptic potential and neuronal excitability,<sup>67,68</sup> they also must be considered as possible candidates that alter cortical excitability after TBI. For example, injury-induced pathology of astrocytic inwardly rectifying K<sup>+</sup> channels have been shown to persist to at least 4 weeks in the neocortex after FPI and is associated with hyperexcitability and post-traumatic epilepsy.<sup>66</sup>

### A cortical rebalancing hypothesis

The chronic shift in the balance of excitation-inhibition toward excitation within the contralesional cortex after injury and reduced ipsilesional activity occurs concurrently with deafferentation across the brain in this model.<sup>20,67,68</sup> One possible mechanism to explain the temporally extended inactivity and hypometabolism that occurs post-injury within the ipsilesional cortex is an increased inhibitory drive from the contralesional hemisphere, in a similar manner to stroke.<sup>69</sup> This would certainly fit with the fact that the degree of ipsilesional-to-contralesional cortex transfer of activation is correlated with injury severity only acutely, because by this hypothesis, the contralesional cortex asserts control via increased excitability at later times to prevent ipsilesional activity. However, further causality-based experimentation is required to provide information to fully support this hypothesis. This may then lay the foundation for future work to determine if neuromodulatory approaches to improving function post-injury occurs through ameliorating cross-brain influences of inhibitory drive onto damaged regions closer to the primary insult, in a manner similar to that used after stroke to alter hemispheric differences in excitability.<sup>70</sup>

There are limitations to this study. First, behavioral analysis of sensorimotor function was not conducted on these animals so that interpretation of the imaging data was made with reliance upon prior functional outcome data acquired by this lab in this model. Second, unlike the fMRI or c-FOS data, rats used for SEP analysis were not investigated for injury severity measures by either MRI or postmortem analyses. This reduced our ability to more closely integrate the data across modalities.

In conclusion, we have shown that TBI-induced changes in evoked sensorimotor network activity occur dynamically post-injury, with a high degree of dependence on the severity of the injury. Loss of evoked ipsilesional activity was met with a corresponding increase in contralesional activity, as shown by both fMRI and c-FOS immunohistology. Parallel electrophysiologic paired-pulse evidence showed that the remote, contralesional BOLD changes occurred concomitantly with increases in cortical excitability, although much earlier reductions in SEP latency indicate that evoked BOLD activity may not capture earlier changes in reorganization.

### Acknowledgments

We wish to thank Andrew Frew and the UCLA In Vivo Imaging Centre.

NIH NINDS NS091222 & NS065877, The UCLA Brain Injury Research Center. The project described was also supported in part

by the MRI Core of the Semel Institute of Neuroscience at UCLA which is supported by Intellectual Development and Disabilities Research Center grant number U54HD087101-01 from the Eunice Kennedy Shriver National Institute of Child Health and Human Development. The content is solely the responsibility of the authors and does not necessarily represent the official views of the Eunice Kennedy Shriver National Institute of Child Health and Human Development or the National Institutes of Health.

### Author Disclosure Statement

No competing financial interests exist.

### References

- Katz, D.I., Alexander, M.P., and Klein, R.B. (1998). Recovery of arm function in patients with paresis after traumatic brain injury. *Arch. Phys. Med. Rehabil.* 79, 488–93.
- Brown, A.W., Malec, J.F., Diehl, N.N., Englander, J., and Cifu, D.X. (2007). Impairment at rehabilitation admission and 1 year after moderate-to-severe traumatic brain injury: a prospective multi-centre analysis. *Brain Inj.* 21, 673–80.
- Black, K., Zafonte, R., Millis, S., Desantis, N., Harrison-Felix, C., Wood, D., and Mann, N. (2000). Sitting balance following brain injury: does it predict outcome? *Brain Inj.* 14, 141–52.
- Hillier, S.L., Sharpe, M.H., and Metzger, J. (1997). Outcomes 5 years post-traumatic brain injury (with further reference to neurophysical impairment and disability). *Brain Inj.* 11, 661–75.
- Wallen, M.A., Mackay, S., Duff, S.M., McCartney, L.C., and O'Flaherty, S.J. (2001). Upper-limb function in Australian children with traumatic brain injury: a controlled, prospective study. *Arch. Phys. Med. Rehabil.* 82, 642–649.
- Walker, W.C. and Pickett, T.C. (2007). Motor impairment after severe traumatic brain injury: A longitudinal multicenter study. *J. Rehabil. Res. Dev.* 44, 975–982.
- Tremblay, S., Beaumont, L. De, Lassonde, M., The, H., de Beaumont, L., Lassonde, M., and Théoret, H. (2011). Evidence for the specificity of intracortical inhibitory dysfunction in asymptomatic concussed athletes. *J. Neurotrauma* 28, 493–502.
- Gagnon, I., Forget, R., Sullivan, S.J., and Friedman, D. (1998). Motor performance following a mild traumatic brain injury in children: an exploratory study. *Brain Inj.* 12, 843–853.
- Haaland, K.Y., Temkin, N., Randahl, G., and Dikmen, S. (1994). Recovery of simple motor skills after head injury. *J. Clin. Exp. Neuropsychol.* 16, 448–456.
- De Beaumont, L., Théoret, H., Mongeon, D., Messier, J., Leclerc, S., Tremblay, S., Ellemerg, D., and Lassonde, M. (2009). Brain function decline in healthy retired athletes who sustained their last sports concussion in early adulthood. *Brain* 132, 695–708.
- Di Russo, F., Incoccia, C., Formisano, R., Sabatini, U., and Zoccolotti, P. (2005). Abnormal motor preparation in severe traumatic brain injury with good recovery. *J. Neurotrauma* 22, 297–312.
- Lotze, M., Markert, J., Sauseng, P., Hoppe, J., Plewnia, C., and Gerloff, C. (2006). The role of multiple contralesional motor areas for complex hand movements after internal capsular lesion. *J. Neurosci.* 26, 6096–6102.
- Bestmann, S., Swayne, O., Blankenburg, F., Ruff, C.C., Teo, J., Weiskopf, N., Driver, J., Rothwell, J.C., and Ward, N.S. (2010). The role of contralesional dorsal premotor cortex after stroke as studied with concurrent TMS-fMRI. *J. Neurosci.* 30, 11926–11937.
- Wu, H.-M., Huang, S.-C., Hattori, N., Glenn, T.C., Vespa, P.M., Hovda, D.A., and Bergsneider, M. (2004). Subcortical white matter metabolic changes remote from focal hemorrhagic lesions suggest diffuse injury after human traumatic brain injury. *Neurosurgery* 55, 1306–1315.
- Harris, N.G., Chen, S.F., and Pickard, J.D. (2013). Cortical reorganisation after experimental traumatic brain injury: a functional autoradiography study. *J. Neurotrauma* 30, 1137–1146.
- Le Priault, F., Thal, S.C., Engelhard, K., Imbrosci, B., Mittmann, T., Priault, F. Le, Thal, S.C., Engelhard, K., and Imbrosci, B. (2016). Acute cortical transhemispheric diaschisis after unilateral traumatic brain injury. *J. Neurotrauma* 14, 1–14.
- Harris, N.G., Verley, D.R., Gutman, B.A., Thompson, P.M., Yeh, H.J., and Brown, J.A. (2016). Disconnection and hyper-connectivity underlie reorganization after TBI: a rodent functional connectomic analysis. *Exp. Neurol.* 277, 124–138.
- Harris, N.G., Nogueira, M.S., Verley, D.R., and Sutton, R.L. (2013). Chondroitinase enhances cortical map plasticity and increases functionally active sprouting axons after brain injury. *J. Neurotrauma* 30, 1257–1269.
- Harris, N.G., Carmichael, S.T., Hovda, D.A., and Sutton, R.L. (2009). Traumatic brain injury results in disparate regions of chondroitin sulfate proteoglycan expression that are temporally limited. *J. Neurosci. Res.* 87, 2937–2950.
- Harris, N.G., Verley, D.R., Gutman, B.A., and Sutton, R.L. (2016). Bi-directional changes in fractional anisotropy after experiment TBI: disorganization and reorganization? *Neuroimage* 133, 129–143.
- Williams, K.A., Magnuson, M., Majeed, W., LaConte, S.M., Peltier, S.J., Hu, X., and Keilholz, S.D. (2010). Comparison of  $\alpha$ -chloralose, medetomidine and isoflurane anesthesia for functional connectivity mapping in the rat. *Magn. Reson. Imaging* 28, 995–1003.
- Woolrich, M. (2008). Robust group analysis using outlier inference. *Neuroimage* 41, 286–301.
- Smith, S.M., Jenkinson, M., Woolrich, M.W., Beckmann, C.F., Behrens, T.E.J.J., Johansen-Berg, H., Bannister, P.R., De Luca, M., Drobnjak, I., Flitney, D.E., Niazy, R.K., Saunders, J., Vickers, J., Zhang, Y., De Stefano, N., Brady, J.M., and Matthews, P.M. (2004). Advances in functional and structural MR image analysis and implementation as FSL. *Neuroimage* 23 Suppl 1, S208–S219.
- Jenkinson, M., Bannister, P., Brady, M., and Smith, S. (2002). Improved optimization for the robust and accurate linear registration and motion correction of brain images. *Neuroimage* 17, 825–841.
- Woolrich, M.W., Behrens, T.E.J., Beckmann, C.F., Jenkinson, M., and Smith, S.M. (2004). Multilevel linear modelling for fMRI group analysis using Bayesian inference. *Neuroimage* 21, 1732–1747.
- Woo, C.W., Krishnan, A., and Wager, T.D. (2014). Cluster-extent based thresholding in fMRI analyses: Pitfalls and recommendations. *Neuroimage* 91, 412–419.
- Eklund, A., Nichols, T.E., and Knutsson, H. (2017). Cluster failure: why fMRI inferences for spatial extent have inflated false-positive rates. *Front. Hum. Neurosci.* 11, 345.
- Hua, X., Gutman, B., Boyle, C.P., Rajagopalan, P., Leow, A.D., Yanovsky, I., Kumar, A.R., Toga, A.W., Jack, C.R., Schuff, N., Alexander, G.E., Chen, K., Reiman, E.M., Weiner, M.W., and Thompson, P.M. (2011). Accurate measurement of brain changes in longitudinal MRI scans using tensor-based morphometry. *Neuroimage* 57, 5–14.
- Meintjes, E.M., Narr, K.L., der Kowze, A.J.W. van, Molteno, C.D., Pirnia, T., Gutman, B., Woods, R.P., Thompson, P.M., Jacobson, J.L., and Jacobson, S.W. (2014). A tensor-based morphometry analysis of regional differences in brain volume in relation to prenatal alcohol exposure. *NeuroImage Clin.* 5, 152–160.
- Dinov, I., Van Horn, J.D., Lozev, K.M., Magsipoc, R., Petrosyan, P., Liu, Z., Mackenzie-Graham, A., Eggert, P., Parker, D.S., and Toga, A.W. (2009). Efficient, distributed and interactive neuroimaging data analysis using the LONI pipeline. *Front. Neuroinform.* 3, 22.
- Tustison, N.J., Avants, B.B., Cook, P.A., Yuanjie Zheng, Y., Egan, A., Yushkevich, P.A., Gee, J.C., Zheng, Y., Egan, A., Yushkevich, P.A., and Gee, J.C. (2010). N4ITK: improved N3 bias correction. *Trans. Med. Imaging* 29.
- R Foundation for Statistical Computing. (2016). R: A language and environment for statistical computing. Available at: [www.R-project.org](http://www.R-project.org). Accessed June 5, 2018.
- Harris, N.G., Mironova, Y.A., Hovda, D.A., and Sutton, R.L. (2010). Chondroitinase ABC enhances pericontusion axonal sprouting but does not confer robust improvements in behavioral recovery. *J. Neurotrauma* 27, 1–12.
- Bütefisch, C.M., Netz, J., Wessling, M., Seitz, R.J., Hömberg, V., Bütefisch, C.M., Netz, J., Wessling, M., Seitz, R.J., and Homberg, V. (2003). Remote changes in cortical excitability after stroke. *Brain* 126, 470–481.
- Duarte, M.N., Just, N., Sonny, S., Gruetter, R., Duarte, J.M., Just, N., and Gruetter, R. (2016). Compartmentalised energy metabolism supporting glutamatergic neurotransmission in response to increased activity in the rat cerebral cortex: a <sup>13</sup>C MRS study in vivo at 14.1 T. *J. Cereb. Blood Flow Metab.* 36, 928–940.
- Zhuo, J., Xu, S., Proctor, J.L., Mullins, R.J., Simon, J.Z., Fiskum, G., and Gullapalli, R.P. (2012). Diffusion kurtosis as an in vivo imaging



- marker for reactive astrogliosis in traumatic brain injury. *Neuroimage* 59, 467–477.
37. Harris, N.G., Chen, S.F., and Pickard, J.D. (2003). Reorganisation after experimental traumatic brain injury: a functional autoradiography study. *J. Cereb. Blood Flow Metab.* 21, 1318.
  38. Shaw, N.A. and Cant, B.R. (1984). The effect of experimental concussion on somatosensory evoked potentials. *Aust. J. Exp. Biol. Med. Sci.* 62 (Pt 3), 361–71.
  39. Johnstone, V.P.A., Shultz, S.R., Yan, E.B., O'Brien, T.J., and Rajan, R. (2014). The acute phase of mild traumatic brain injury is characterized by a distance-dependent neuronal hypoactivity. *J. Neurotrauma* 31, 1881–1895.
  40. Dietrich, W.D., Alonso, O., Busto, R., and Ginsberg, M.D. (1994). Widespread metabolic depression and reduced somatosensory circuit activation following traumatic brain injury in rats. *J. Neurotrauma* 11, 629–640.
  41. Moro, N., Ghavim, S.S., Hovda, D.A., and Sutton, R.L. (2011). Delayed sodium pyruvate treatment improves working memory following experimental traumatic brain injury. *Neurosci. Lett.* 491, 158–162.
  42. Cantu, D., Walker, K., Andresen, L., Taylor-Weiner, A., Hampton, D., Tesco, G., and Dulla, C.G. (2014). Traumatic brain injury increases cortical glutamate network activity by compromising GABAergic control. *Cereb. Cortex* 25, 2306–2320.
  43. Ip, E.Y., Zanier, E.R., Moore, A.H., Lee, S.M., and Hovda, D.A. (2003). Metabolic, neurochemical, and histologic responses to vibrissa motor cortex stimulation after traumatic brain injury. *J. Cereb. Blood Flow Metab.* 23, 900–910.
  44. Holschneider, D.P., Guo, Y., Wang, Z., Roch, M., and Scremin, O.U. (2013). Remote brain network changes after unilateral cortical impact injury and their modulation by acetylcholinesterase inhibition. *J. Neurotrauma* 30, 907–919.
  45. Dijkhuizen, R.M., Singhal, A.B., Mandeville, J.B., Wu, O., Halpern, E.F., Finklestein, S.P., Rosen, B.R., and Lo, E.H. (2003). Correlation between brain reorganization, ischemic damage, and neurologic status after transient focal cerebral ischemia in rats: a functional magnetic resonance imaging study. *J. Neurosci.* 23, 510–517.
  46. Imbrosci, B., Ytebrouck, E., Arckens, L., and Mittmann, T. (2014). Neuronal mechanisms underlying transhemispheric diaschisis following focal cortical injuries. *Brain Struct. Funct.* 220, 1649–1664.
  47. Cramer, S.C., Nelles, G., Benson, R.R., Kaplan, J.D., Parker, R.A., Kwong, K.K., Kennedy, D.N., Finklestein, S.P., and Rosen, B.R. (1997). A functional MRI study of subjects recovered from hemiparetic stroke. *Stroke* 28, 2518–2527.
  48. Hsu, J.E. and Jones, T.A. (2005). Time-sensitive enhancement of motor learning with the less-affected forelimb after unilateral sensorimotor cortex lesions in rats. *Eur. J. Neurosci.* 22, 2069–2080.
  49. Hsu, J.E. and Jones, T.A. (2006). Contralateral neural plasticity and functional changes in the less-affected forelimb after large and small cortical infarcts in rats. *Exp. Neurol.* 201, 479–494.
  50. Nita, D.A., Cisse, Y., Timofeev, I., Steriade, M., Dragos, A., Cisse, Y., Timofeev, I., Cissé, Y., Timofeev, I., Steriade, M., Nita, D.A., Cisse, Y., Timofeev, I., and Steriade, M. (2007). Increased propensity to seizures after chronic cortical deafferentation in vivo. *J. Neurophysiol.* 95, 902–913.
  51. Avramescu, S. and Timofeev, I. (2008). Synaptic strength modulation after cortical trauma: a role in epileptogenesis. *J. Neurosci.* 28, 6760–6772.
  52. Allred, R.P., Cappellini, C.H., and Jones, T.A. (2010). The “good” limb makes the “bad” limb worse: experience-dependent interhemispheric disruption of functional outcome after cortical infarcts in rats. *Behav. Neurosci.* 124, 124–132.
  53. Reeves, T.M., Lyeth, B.G., Phillips, L.L., Hamm, R.J., and Povlishock, J.T. (1997). The effects of traumatic brain injury on inhibition in the hippocampus and dentate gyrus. *Brain Res.* 757, 119–132.
  54. Hunt, R.F., Scheff, S.W., and Smith, B.N. (2009). Posttraumatic epilepsy after controlled cortical impact injury in mice. *Exp. Neurol.* 215, 243–252.
  55. Thomas, J., Smith, H., McIntosh, K., Lowenstein, D.H., Thomas, M.J., Smith, D.H., and McIntosh, T.K. (1992). Selective vulnerability of dentate hilar neurons following traumatic brain injury: a potential mechanistic link between head trauma and disorders of the hippocampus. *J. Neurosci.* 12, 4846–4853.
  56. Golarai, G., Greenwood, A.C., Feeney, D.M., and Connor, J.A. (2001). Physiological and structural evidence for hippocampal involvement in persistent seizure susceptibility after traumatic brain injury. *J. Neurosci.* 21, 8523–8537.
  57. Kang, W.H. and Morrison, B. (2014). Functional tolerance to mechanical deformation developed from organotypic hippocampal slice cultures. *Biomech. Model Mechanobiol.* 14, 561–575.
  58. Hunt, R.F., Scheff, S.W., Smith, B.N., Hunt, R.F., Scheff, S.W., Smith, B.N., Hunt, R.F., Scheff, S.W., and Smith, B.N. (2012). Regionally localized recurrent excitation in the dentate gyrus of a cortical contusion model of posttraumatic epilepsy regionally localized recurrent excitation in the dentate gyrus of a cortical contusion model of posttraumatic epilepsy. 103, 1490–1500.
  59. Katayama, Y., Becker, D.P., Tamura, T., and Hovda, D.A. (1990). Massive increases in extracellular potassium and the indiscriminate release of glutamate following concussive brain injury. *J. Neurosurg.* 73, 889–900.
  60. Richards, H.K., Bucknall, R.M., Jones, H.C., and Pickard, J.D. (1995). Uncoupling of LCBF and LCGU in two different models of hydrocephalus: a review. *Childs Nerv. Syst.* 11, 288–292.
  61. Kawamata, T., Katayama, Y., Hovda, D.A., Yoshino, A., and Becker, D.P. (1992). Administration of excitatory amino acid antagonists via microdialysis attenuates the increase in glucose utilization seen following concussive brain injury. *J. Cereb. Blood Flow Metab.* 12, 12–24.
  62. Hånell, A., Greer, J.E., and Jacobs, K.M. (2015). Increased network excitability due to altered synaptic inputs to neocortical layer V intact and axotomized pyramidal neurons after Mild Traumatic Brain Injury. *J. Neurotrauma* 32, 1590–1598.
  63. Porter, J.T., and Nieves, D. (2004). Presynaptic GABA B receptors modulate thalamic excitation of Inhibitory and Excitatory neurons in the mouse barrel cortex. *J. Neurophysiol.* 92, 2762–2770.
  64. Metherate, R. and Ashe, J.H. (1994). Facilitation of an NMDA receptor-mediated EPSP by paired-pulse stimulation in rat neocortex via depression of GABAergic IPSPs. *J. Physiol.* 481 (Pt 2), 331–348.
  65. Dobrunz, L.E. and Stevens, C.F. (1997). Heterogeneity of release probability, facilitation, and depletion at central synapses. *Neuron* 18, 995–1008.
  66. Stewart, T.H., Eastman, C.L., Groblewski, P.A., Fender, J.S., Verley, D.R., Cook, D.G., Ambrosio, R.D., D'Ambrosio, R., and Ambrosio, R.D. (2010). Chronic dysfunction of astrocytic inwardly rectifying K<sup>+</sup> channels specific to the neocortical epileptic focus after fluid percussion injury in the rat. *J. Neurophysiol.* 104, 3345–3360.
  67. Hall, E.D., Bryant, Y.D., Cho, W., and Sullivan, P.G. (2008). Evolution of post-traumatic neurodegeneration after controlled cortical impact traumatic brain injury in mice and rats as assessed by the de Olmos silver and fluorojade staining methods. *J. Neurotrauma* 25, 235–247.
  68. Matthews, M.A., Carey, M.E., Soblosky, J.S., Davidson, J.F., and Tabor, S.L. (1998). Focal brain injury and its effects on cerebral mantle, neurons, and fiber tracks. *Brain Res.* 794, 1–18.
  69. Murase, N., Duque, J., Mazzocchio, R., and Cohen, L.G. (2004). Influence of interhemispheric interactions on motor function in chronic stroke. *Ann. Neurol.* 55, 400–409.
  70. Barry, M.D., Boddington, L.J., Igelström, K.M., Gray, J.P., Shemmell, J., Tseng, K.Y., Oorschot, D.E., and Reynolds, J.N.J. (2014). Utility of intracerebral theta burst electrical stimulation to attenuate interhemispheric inhibition and to promote motor recovery after cortical injury in an animal model. *Exp. Neurol.* 261, 258–266.

Address for correspondence:

*Neil G. Harris, PhD*

*UCLA Brain Injury Research Center*

*Department of Neurosurgery*

*David Geffen School of Medicine at UCLA*

*300 Stein Plaza, Suite 535, Box 956901*

*Los Angeles, CA 90095*

*E-mail: ngharris@ucla.edu*